Dynamic Orientation Sensing for AR using a Model-based Relative Acceleration Method

Matthew S. Keir[†,*,1], Chris E. Hann[†], J. Geoffrey Chase[†] and XiaoQi Chen[†]

[†]Mechanical Engineering Department
University of Canterbury,
Christchurch, New Zealand

[*]Human Interface Technology Lab
University of Canterbury,
Christchurch, New Zealand

ABSTRACT

Accurate viewpoint tracking for Augmented Reality applications is a challenging task. This paper presents a new model-based approach to tracking dynamic orientation using accelerometers. However, the inverted pendulum model applied consists of an unstable coupled set of differential equations which cannot be solved by conventional solution approaches. A unique method is developed which allows a separation of the unstable transient part of the solution from the stable solution leaving the required orientation. The methods are validated experimentally for dynamic translation and rotation in a vertical plane using accelerometer data from an inverted pendulum apparatus. The results are shown to outperform existing state of the art, gyroscope based methods. This proof of concept shows how low-cost accelerometer sensors can potentially to improve head tracking in dynamic AR environments.

1. INTRODUCTION

Augmented reality (AR) systems that use head mounted displays to overlay synthetic imagery on the user's view of the real world, require accurate viewpoint tracking for quality applications. However, achieving accurate registration is one of the most significant unsolved problems within AR systems, particularly during dynamic motions in unprepared environments. As a result, registration error is a major issue hindering more widespread growth of AR applications.

Robust tracking systems are available for quasi-static applications. However, when applied in more dynamic applications they fail to produce the accuracy required. Many different technologies have been applied to the head tracking problem, although no one technology tracks well for all applications [1]. Micro-Electro-Mechanical Systems (MEMS) based inertial sensors have clear advantages for highly dynamic applications:

- They are small in size which allows unobtrusive packaging,
- They are immune to interference and are not restricted by line of sight allowing easy operation in unprepared environments,
- They have high update rates which reduces system latency,
- They are inexpensive compared with other available tracking approaches.

Despite these advantages inertial devices suffer one main problem in determining position or orientation. Rate gyroscope (gyro) signals require integration to obtain orientation and accelerometer signals require double integration to determine position. Numerical integration of these noisy signals causes the results to drift. The effects of orientation drift can be corrected or minimised. However, correcting drift in the position is more difficult. Hence, inertial devices are only useful for tracking orientation in this application. Importantly AR systems are more sensitive to orientation error than position error, as the orientation error is scaled by the distance to the viewed object [2].

Accelerometers sense dynamic accelerations along with the acceleration due to gravity. This ability to sense the gravitational acceleration can be very useful in determining tilt or orientation. For a stationary object finding the orientation with respect to gravity is a trivial problem. However, when other motion is introduced the acceleration signal is modified by the dynamic accelerations, leading to

[1]Corresponding author: Tel.: (+64 3) 364-2987 ext3070; E-mail: matthew.keir@hitlabnz.org.nz

orientation errors. One inertial approach to tracking head motion is to take advantage of the burst like nature of head motion and correct for gyro drift using the accelerometer during natural pauses [3]. Commercial inertial measurement units (IMUs) suitable for tracking 3DOF head motion include, the InertiaCube3 [4], 3d-Bird [5], MTx [6] and the 3DM-DH [7]. These IMUs typically contain three rate gyroscopes, accelerometers and magnetometers. However, these devices are not optimised for individual applications. None are fully proven in a highly dynamic environment.

This paper presents a unique approach to improve orientation tracking of the head in a highly dynamic environment using only dual axis accelerometers. The approach extends the excellent static orientation sensing abilities of accelerometers for pitch and roll orientations to a dynamic case using a model of head motion. This proof of concept considers two dimensional motion, consisting of both rotation and translation degrees of freedom, within a vertical plane. The inverted pendulum model applied is described by two independent non linear differential equations which cannot be solved by conventional methods. A unique approach is presented and validated with experimental results and compared made to a gyroscope and state of the art MEMS IMU.

2. METHOD

An inverted pendulum model applies where a mass is balanced above an axis of rotation. In this application the mass is a human head and this is supported above the shoulders by the cervical spine. This head-neck system is modelled in two dimensions using an inverted pendulum. The model is extended from one rotational degree of freedom as seen in [8] to include translational motion of the centre of rotation. This combined motion represents motion such as the pitch motion of the head while walking.

The schematic shown in Figure 1 for the model includes two dual axis accelerometers. The first accelerometer, denoted Accelerometer 1, is positioned along the pendulum at radius R, aligned in the plane of motion. It has axes denoted $A_{x,1}(t)$ and $A_{y,1}(t)$ orientated at a fixed angle λ_1 to the tangential axis, $A_T(t)$. This accelerometer senses the combined acceleration due to both the rotation and the translation of the centre of rotation. The radius of rotation for the head is assumed to be fixed, although it may be more accurately a function of the rotation.

The second accelerometer, Accelerometer 2, with axes $A_{x,2}(t)$ and $A_{y,2}(t)$ is positioned at fixed angle λ_2 to the horizontal axis, $A_H(t)$. This accelerometer senses the accelerations, $A_h(t)$ and $A_v(t)$, which are due to the horizontal and vertical translational motion of the centre of rotation. Although Accelerometer 2 is shown in Figure 1 at the centre of rotation, it can, in theory, be placed anywhere on the rigid body supporting the pendulum. This placement provides the acceleration at the centre of rotation. Thus, for head tracking, this accelerometer may be placed at the centre of the back inline with the shoulders, within a tight fitting backpack containing other components required for the AR system.

The model resolves acceleration in terms of gravity, g, along each respective axis, tangential A_T, radial A_R, vertical A_V, horizontal A_H, in Figure 1. Measured dynamic accelerations due to tangential, centripetal, A_v and A_h, will contribute in the opposite direction shown in Figure 1 because the accelerometers sense acceleration of the proof mass relative to the casing. All accelerations and rotations $(\theta(t), \dot{\theta}(t))$ are functions of time, but "(t)" is dropped for clarity.

$$A_T = (R/g)\ddot{\theta} - \sin(\theta) - A_h\cos(\theta) - A_v\sin(\theta) \quad (1)$$

$$A_R = (R/g)\dot{\theta}^2 - \cos(\theta) + A_h\sin(\theta) - A_v\cos(\theta) \quad (2)$$

$$A_H = -A_h \quad (3)$$

$$A_V = -A_v - 1 \quad (4)$$

Equations (3) and (4) are limited to the case where λ_2 is constant in Figure 1. However, Equations (1) and (2) provide general model equations for any translation of the centre of rotation.

The actual tangential (A_T), radial (A_R), vertical (A_V) and horizontal (A_H) accelerations are derived

from the measured accelerations of Accelerometers 1 and 2, and are defined:

$$A_T = A_{x,1}\cos(\lambda_1) - A_{y,1}\sin(\lambda_1) \tag{5}$$
$$A_R = A_{x,1}\sin(\lambda_1) + A_{y,1}\cos(\lambda_1) \tag{6}$$
$$A_H = A_{x,2}\cos(\lambda_2) - A_{y,2}\sin(\lambda_2) \tag{7}$$
$$A_V = A_{x,2}\sin(\lambda_2) + A_{y,2}\cos(\lambda_2) \tag{8}$$

A comparison of A_T and A_R from Equations (1) and (2) is made with the experimentally measured A_T and A_R of Equations (5) and (6) in the results to verify that this extended model is valid.

The inverted pendulum model consists of the coupled set of differential Equations (1) and (2), which are unstable and cannot be solved by conventional approaches. The method presented is based on fitting the model over a short period to determine the next θ value, denoted θ_{new} in Figure 2(B). Note that the method accurately determines the orientation θ in the presence of a disruptive translation to the centre of rotation. However, the method is not concerned with determining the translation itself.

The A_h and A_v parameters are found by rearranging Equations (3) and (4) in terms of A_H and A_V, which are derived directly from the measured accelerations of Accelerometer 2 in Equations (7) and (8). A piecewise linear expression is developed by substituting linear approximations over each sample step of length Δt for the acceleration and trigonometric terms into Equation (1). The accelerations, A_T, A_h, and A_v are linearised in terms of time, as seen in Figure 2(A) for A_T. The trigonometric terms, $\sin(\theta)$ and $\cos(\theta)$, are linearised in terms of θ across the range of theta in each section of length Δt from the past θ values. Collecting terms gives a linear, non homogeneous differential equation:

$$(R/g)\ddot{\theta} + E(t)\theta = F(t) \tag{9}$$

where for the ith section:

$$\begin{aligned} E(t) &= E_{1,i} + E_{2,i}t \qquad t_{i-1} \leqslant t \leqslant t_i \\ F(t) &= F_{1,i} + F_{2,i}t \qquad t_{i-1} \leqslant t \leqslant t_i \qquad i = 1, ..., k \end{aligned} \tag{10}$$

Linear coefficients $E_{1,i}$, $E_{2,i}$, $F_{1,i}$, and $F_{2,i}$ are found by summing the linear coefficients of each contributing variable.

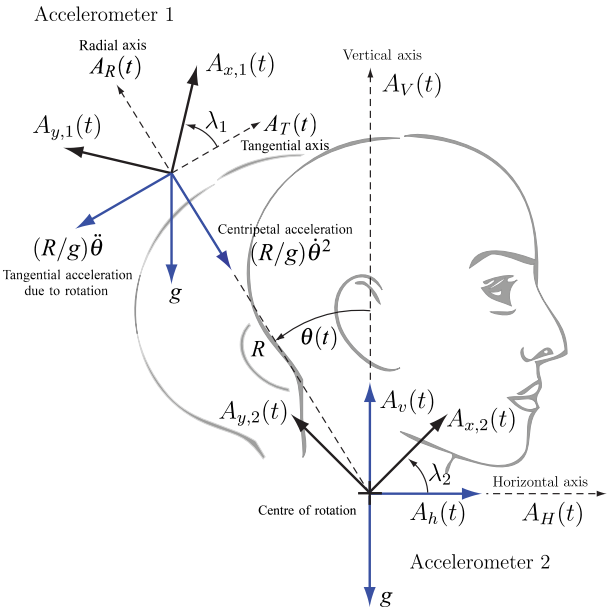

Figure. 1: Schematic of the extended inverted pendulum model, including rotation and translation of the centre of rotation in a 2 dimensional plane

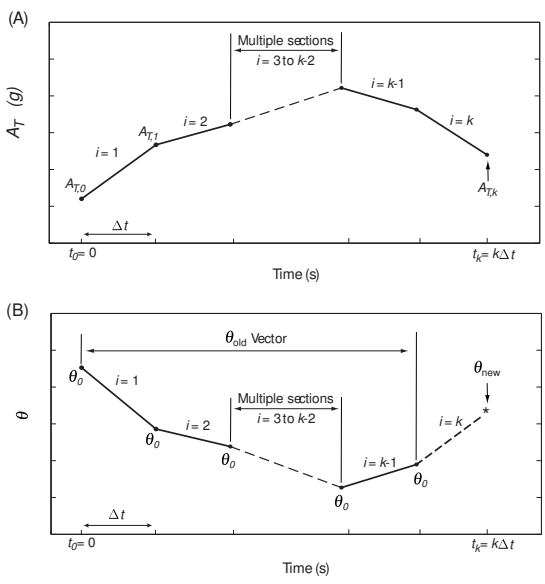

Figure. 2: (A) The linearisation of the measured tangential acceleration, A_T, between measured points; (B) The θ value derived at each measurement point. Note, that past values are stored in a vector θ_{old}, and θ_{new} denotes the unknown θ value for the current time point

For the case of one rotational degree of freedom, achieved by setting $A_h = 0$ and $A_v = 0$ in Equation (1), an accurate closed form analytical solution was constructed in terms of an arbitrary set of initial

conditions [8]. The solution for θ was then found using the second independent radial Equation (2) to select optimal initial conditions. In the case where $A_h \neq 0$ and $A_v \neq 0$, an analytical solution to Equation (9) does not exist. However, an analytical solution does exist to the homogeneous equation, which is derived by setting $F(t) = 0$ in Equation (9). The resulting equation is defined:

$$(R/g)\ddot{\theta} + (E_{1,i} + E_{2,i}t)\theta = 0 \qquad i = 1, ..., k \tag{11}$$

The analytical solution to Equation (11) can be readily computed in Maple$^{\text{TM}}$ and is defined:

$$y_{c,i}(t) = C_1 AiryAi(M_i) + C_2 AiryBi(M_i) \qquad i = 1, ..., k \tag{12}$$

where:

$$M_i = \left(- \frac{E_{2,i}^{1/3}\big(E_{1,i} + E_{2,i}(t)\big)}{E_{2,i}R^{1/3}} \right) \tag{13}$$

and C_1 and C_2 are unknown constants, and $AiryAi$ and $AiryBi$ are wave functions related to Bessel functions that are built into both Maple$^{\text{TM}}$ and Matlab$^{\text{TM}}$.

The standard solution to a linear non homogeneous ODE is a linear combination of the complementary and particular solutions. Following this standard theory, the solution is constructed as follows.

$$\theta_{sol,i} = y_{c,i}(t) + y_p(t) \qquad i = 1, ..., k \tag{14}$$

where $y_{c,i}(t)$ is the the complementary solution of Equation (11) and $y_p(t)$ is a particular solution to the linear ODE in Equation (9). The complementary solution $y_{c,i}(t)$ in Equation (14) represents the transient response and only applies over ith section defined by the period $t_{i-1} < t < t_i$. The particular solution $y_p(t)$ is a numerical solution of the full linear ODE of Equation (9) with essentially arbitrary initial conditions. For simplicity, these initial conditions are set to zero.

In many engineering problems the particular solution $y_p(t)$ represents the steady state solution, which is independent of the initial conditions. The problem in this case is that $y_p(t)$ is highly sensitive to initial conditions, as the transient solution $y_c(t)$ in Equation (14) does not die away. If the initial conditions for $\theta_{sol,i}$ are known precisely there is no need for $y_{c,i}(t)$ in Equation (14). However, initial conditions are never known precisely in practice. It is thus vital to separate the solutions $y_{c,i}(t)$ and $y_p(t)$ to accurately determine $\theta_{sol,i}$ in Equation (14). A further fundamental point is that the underlying differential equation must be linear to allow a solution of the form of Equation (14). This point emphasises the importance of the formulation of Equation (9), as no such construction can be applied to the non linear model of Equations (1) and (2).

A recursive solution is developed for θ_{sol}, in Equation (14), where the initial conditions of $y_{c,i}(t)$ are defined by $y_{c,i-1}(t_{i-1})$, the expression at the end the previous section, in terms of the unknown initial conditions for the first section θ_0 and $\dot{\theta}_0$. Due to space restrictions the full recursive expression is not shown. The expression θ_{sol} is substituted into Equation (2) and the optimal initial conditions, θ_0 and $\dot{\theta}_0$, determined by fitting the expression to the the measured radial acceleration from Equation (6). Substituting the optimal initial conditions into Equation (14) and evaluating the solution at the end of the fit period $t = t_k$, provides θ_{new} for the current time step. The vector θ_{old} is then updated and the process repeated for the next time step.

3. RESULTS

An experiment was undertaken using a physical inverted pendulum apparatus. Optical encoders provided an independent measure of rotation and horizontal cart position. The rotational measure was compared to the accelerometer based method presented, a gyroscope, and an Inertia Cube 3 used with zero heading and enhancement set to option 2. Experimental measurements were collected by manually moving the cart and pendulum.

Figure 3(b) shows the cart displacement and total acceleration, A_H and A_V, for a 10 second period. The cart displacement of approximately 15cm is measured using the optical encoder attached to the cart running to the track, and A_H and A_V are derived from the Accelerometer 2 measurement in Equations (7) and (8). Figure 3(a) shows the comparison of A_T and A_R derived from the model Equations (1)

and (2) with the measured values from Accelerometer 1 in Figure 1 and Equations (5) and (6). A_T shows a good fit, with 4.6% mean absolute error. However, A_R suffers from poor signal quality when near vertical giving 20.7% mean absolute error. These results confirm the validity of the model to this experimental set up.

The method is applied over the 10 second, 100Hz sampled signal with the period in the algorithm set to 0.45s or the number of sample steps $k = 45$. The accelerometer method results are compared to results from the Inertia Cube 3 and an Analogue Devices ADXRS150 gyroscope in Figure 3(c) and the absolute error in Figure 3(d). These results are summarised by the absolute error metrics in Table 1.

Table 1: Accelerometer method experimental error results for the 10 second signal

Device/Method	Max (deg)	STD (deg)	Mean (deg)	%
Accelerometer Method	1.63	0.30	0.36	3.82
Inertia Cube 3	1.62	0.41	0.61	6.58
Gyroscope	3.24	0.79	1.08	11.06

The accelerometer method outperforms the Inertia Cube 3 and gyroscope for this signal. More specifically, a mean absolute percentage error of 3.82% is achieved, compared with 6.58% and 11.06% for the Inertia Cube 3 and gyroscope respectively.

4. CONCLUSION

The accelerometer model-based method presented in this paper clearly shows that accurate orientation can be determined for the inverted pendulum model of head motion while undergoing dynamic rotation and translation of the pivot in a single vertical plane. This case and method cover a far more general scenario then the single rotational degree of freedom case presented in [8], and [9]. It also provides an approach that can be readily generalised to other vertical head motion planes, and thus extended to three dimensions, providing potential for improved head tracking for dynamic AR applications.

References

[1] G. Welch and E. Foxlin, "Motion tracking: No silver bullet, but a respectable arsenal," IEEE Computer Graphics and Applications*, vol. 22, no. 6, pp. 24–38, 2002.*

[2] R. L. Holloway, "Registration error analysis for augmented reality," Presence: Teleoperators and Virtual Environments*, vol. 6, no. 4, pp. 413–432, 1997.*

[3] E. Foxlin, M. Harrington, and Y. Altshuler, "Miniature 6-DOF inertial system for tracking HMDs," in Proceedings of the SPIE*, vol. 3362, Orlando, FL, 1998, pp. 214–228.*

[4] Inetersense Inc, "Home page," http://www.isense.com/, 2007, 1/8/ 2007.

[5] Ascension Technology Corporation, "Home page," http://www.ascension-tech.com/, 2007,

[6] Xsens Technology, "Home page," http://www.xsens.com/, 2007, 1/8/ 2007.

[7] Micro Strain, "Home page," http: //www.microstrain.com/, 2007, 1/8/ 2007.

[8] M. S. Keir, C. E. Hann, J. G. Chase, and X. Q. Chen, "Accelerometer-based orientation sensing for head tracking in AR & robotics," in Proceedings of The 2nd International Conference on Sensing Technology (ICST 2007)*, Palmerston North, New Zealand, 2007.*

[9] M. S. Keir, C. E. Hann, J. G. Chase, and X. Q. Chen, "A new approach to accelerometer-based head tracking for augmented reality & other applications," in Proceedings of the IEEE Ineernational Conference on Automation Science and Engineering (CASE 2007)*, Scottsdale, AZ, USA, 2007, pp. 603–608.*

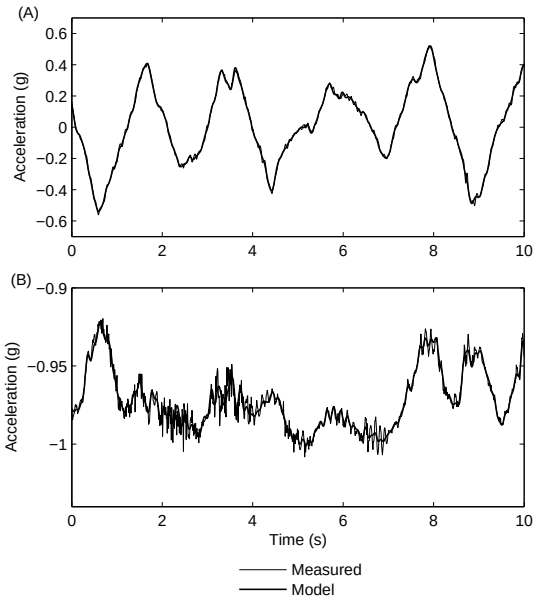

(a) Model validation, measured and model accelerations: (A) Tangential acceleration, A_T; (B) Radial acceleration, A_R

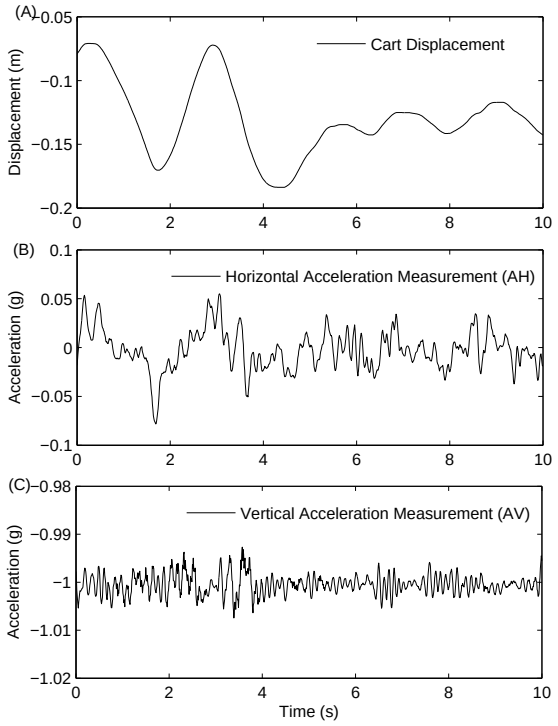

(b) Cart displacement and total acceleration: (A) Measured displacement via cart encoder; (B) Measured horizontal acceleration, A_H, via Accelerometer 2 and Equation (7); (C) Measured vertical acceleration, A_V, via Accelerometer 2 and Equation (8)

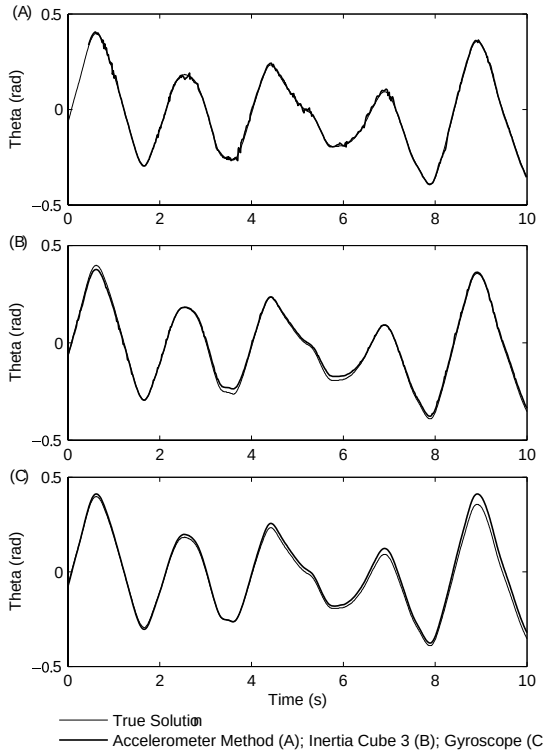

(c) Experimental comparisons to determining orientation, θ, using the Accelerometer Method (A), Inertia Cube 3 (B), and Gyroscope (C)

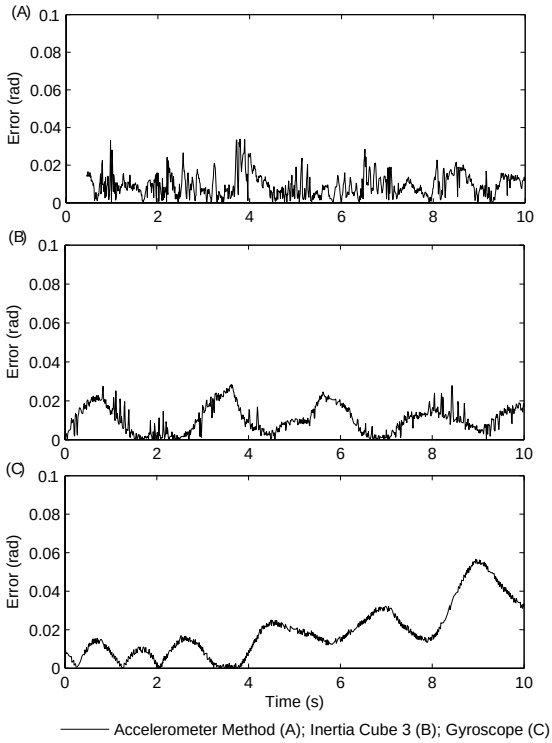

(d) Absolute error in θ for the signal and solution methods of Figure 3(c). The Accelerometer Method (A), Inertia Cube 3 (B), and Gyroscope (C)

Figure. 3: Experimental Results